Fluid flow phenomena in bottom gas-stirred ladles with top layer : Part II. Practical considerations

Fluid flow phenomena in bottom gas-stirred ladles with top layer: Part II. Practical considerations

By Alberto N. Conejo[*1], Shin-ya Kitamura[*2]

In order to define the optimum number and location of injection devices to optimize fluid flow in metallurgical ladles it is necessary to understand the phenomena associated with bottom gas injection such as mass transfer, mixing, the role of the top layer as well as bubble behavior. The research work carried out in the previous 35 years is reviewed, with special attention to the application of laboratory results to the industrial scale. Part I in this work reviewed the fundamental aspects. This part focuses on practical considerations such as scale-up, the limitations of porous plugs to produce small size bubbles in industrial conditions and a review on the optimum configuration of injection devices.

(Received on December 14th, 2009)

Keywords: *fluid flow, mixing time, ladle eye, mass transfer, gas injection*

1 Introduction

This review has the objective to summarize the progress made on the physical and mathematical modeling of gas stirring in ladles, emphasizing its application to the industrial conditions, in particular on the optimum configuration of injection elements to improve mixing time. In part I the fundamental concepts on fluid flow phenomena involving a top layer are reviewed. Part II will deal with the industrial considerations.

2 Scale up and dynamic similarity between water model and industrial ladle

Water modeling provides information on mixing and mass transfer phenomena in small scale vessels. The resulting information should be used to predict actual events in full scale systems however the current knowledge to scale up that information is very poor. In some way the changes to define dynamic similarity between water model and industrial ladle have also affected the definition of a unified criteria to scale up the results from the water models.

According to Mazumdar [1] in any flow system, the balance between various forces acting on a fluid element can be described by the Navier-Stokes equation. In dimensionless form, this equation involves three dimensionless numbers (Eu, Re, Fr). In principle, dynamic similarity requires to respect both Reynolds (Re) and Froude (Fr) numbers. Because the kinematic viscosity of water at room temperature is similar to that of steel at 1600°C, fluid flow phenomena in isothermal water modeling is considered to be dominated only by inertial and gravitational forces (rather than molecular viscous forces) and therefore, dynamic similarity is achieved when the ratio of the inertial to the buoyancy forces in both systems is similar. As the gas is discharged through the orifice into the surrounding heavier liquid, it expands quickly due to the sudden pressure drop and temperature change, the duration of this process is found to be about 0.1–0.3 s, according to Hsiao *et al.* [2]. Each bubble exerts a force on its surroundings proportional to its buoyancy. Thus, the liquid around the bubbles is accelerated and moves upwards following the bubbles.

[*1] Morelia Technological Institute（東北大学多元物質科学研究所客員教授）
[*2] 東北大学多元物質科学研究所

The motion is then transferred to the steel bulk near the bubble plume by viscous forces and lateral turbulent fluctuation. When the bubble-liquid mixture reaches the surface, bubbles break trough to the atmosphere, and the momentum of the liquid stream is converted into a radially spreading surface flow. The inertial force involves a velocity scale and a characteristic length and taking into account that the hydrodynamic conditions at the nozzle orifice are not critical to the bulk flow recirculation induced because the kinetic energy of the incoming gas, which is in the order of 5-10%, is considerable less than the potential energy afforded by the rising bubbles, then, the initial velocity cannot be used as the velocity scale in the Froude number. The average recirculation velocity (mean speed) cannot be known apriori. If used as the velocity scale, the dimensionless number would not be physically meaningful, according to Mazumdar. Based on the previous arguments, the correct velocity scale in the ladle Froude number is the plume velocity, as follows:

$$Fr = \frac{U_p^2}{gH} \tag{1}$$

Where: Fr is the Froude number, U_p is the plume velocity, g is the gravity constant and H the height of the liquid.

The first derived equation to compute plume velocity was reported by Sahai and Guthrie [3,4], they also observed that center line velocities are about 25% higher than the average plume velocity in 250t industrial ladles. Mazumdar *et al.* [5,6] reported two additional relationships for the plume velocity also as a function of gas flow rate and ladle dimensions. Once the equation for the plume velocity is obtained, it is inserted into the ladle Froude number to derive a relationship between gas flow rate in the water model and full scale system, as follows.

$$Fr_m = Fr_{f_s} \tag{2}$$

$$Q_m = \lambda^n Q_{f_s} \tag{3}$$

Where: Fr_m is the ladle Froude number for the water model, Fr_{f_s} is the ladle Froude number for the industrial ladle or full scale system, λ is the aspect ratio (defined as $H_m/H_{f_s} = R_m/R_{f_s}$) and "$n$" is an exponent.

Equation (3) is the basis to satisfy dynamic similarity and to design a water model. The first relationship was reported by Mazumdar and Guthrie [7], however instead of the plume velocity they used the average recirculation velocity, obtaining an exponent equal to 2.75. When they introduced the plume velocity, the exponent was reported as 1.5. The large variation in the magnitude of the exponent affects the decision of the true gas flow rate in the water model to achieve dynamic similarity. Kim and Fruehan [8] also derived a scaling equation, using the velocity at the nozzle an not the plume velocity, obtaining an exponent of 2.5. Sudhakar and Mazumdar [9] have criticized the use of a modified Froude number in

Table 1 Plume velocity and magnitude of exponent n.

Year	Authors	Plume velocity	n
1982	Y. Sahai and R. Guthrie [3]	$U_p = 4.4Q^{\frac{1}{3}}H^{\frac{1}{4}}R^{-\frac{1}{3}}$	-
1985	D. Mazumdar and R.Guthrie [7]	$\overline{U}$	2.75
1987	Kim and Fruehan [8]	$U_n = \frac{Q_n}{\pi d_n^2/4}$	2.5
1993	D. Mazumdar *et.al.* [5]	$U_p = 4.5Q^{\frac{1}{3}}H^{\frac{1}{4}}R^{-\frac{1}{4}}$	1.5
2002	D. Mazumdar [6]	$U_p = 3.1Q^{0.33}H^{0.25}R^{-0.58}$	2.5
U_p[m/s], H[m], R[m], U_n[cm/s], Q_n[l/min], d_n[cm]			

terms of the nozzle velocity, however Kim and Fruehan's analysis appears to contradict such criticism. Mazumdar *et al.* [10] reviewed the validity of the three exponents, 1.5, 2.5 and 2.75, reporting better predictions of the experimental results using the value of 2.5. Subsequently, Mazumdar [6] also reported a new equation for the plume velocity which allowed the definition of the exponent as 2.5. This exponent appears to be the accepted one in current designs of water models. It is important to mention that the gas flow rate in the full scale system corresponds to the liquid steel temperature and average pressure at the half of the height depth. Table 1 summarizes the values reported for the exponent "n" in Equation (3).

The knowledge on mixing time for industrial conditions is very poor. Mazumdar *et al.* [1, 11, 12] applied the ratio of gas flow rates between model and full scale system to define a ratio for mixing times. The final equation was similar as that for the ratio between gas flow rates($\tau_{f_s} = \lambda^{-n}\tau_m$). The exponent was reported progressively as 4/3, 5/6 and finally as 1/2. Neifer *et al.* [13] included a similar relationship including the ratio between the density of the gas under standard conditions and its average density under operating conditions. Asai *et al.* [14] included a ratio of densities between iron and water, which gives a value of 1.9. Considering that the order of magnitude of mixing time in water models is typically in the range from 50-100 seconds, multiplying by a factor of two as Asai suggests appears to be small for industrial conditions.Ogawa and Onoue [15] also reported a relationship between mixing time and stirring energy for liquid steel, where the proportionality constant was given in terms of the volume of steel. Abel *et al.* [16] proposed a practical approach. They compared mixing time for water models and for industrial conditions. Mixing time was related exclusively with stirring energy. The relationship between mixing time and stirring energy has the form, $\tau_m = C\dot{\varepsilon}^{-0.36}$. The coefficient was about 80 for water models and 800 for industrial conditions; this gives a difference of one order of magnitude between model and full scale system. Figure 1 shows the comparison of mixing times between water models and industrial conditions based on the results by Abel *et al.* [16].

The authors argued that ladle dimensions and mode of injection affect mixing time but only at low gas flow rates. At high gas flow rates ($> 110\ l/\mathrm{min}$) there is no influence of bath height and tuyere pattern on mixing time. This conclusion refutes one of the previous arguments by Mazumdar and Guthrie [11].

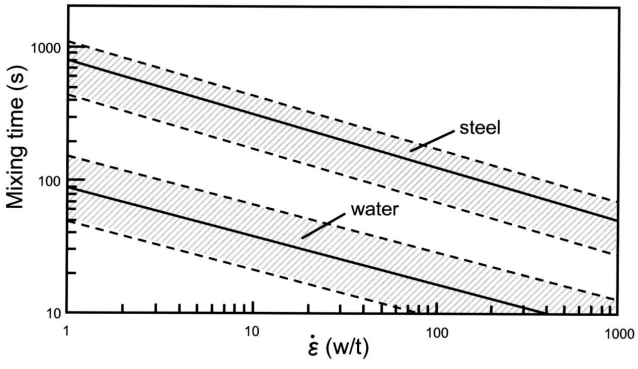

Fig.1 Difference of the relation between mixing time and stirring intensity in water model and industrial vessel based on ref. [16].

3 Fluid flow phenomena in ladles agitated with nozzles and porous plugs

Bubble size measured in water models is not truly representative of the bubble size obtained in industrial conditions due to two factors [17]; (i) wettability between water and liquid steel

with porous plugs is very different, (ii) bubble thermal expansion is not taken into account in water models. Wang *et al.* [18] reported experimental values of contact angles. The contact angle between porous plugs and water was reported as 16.8° and that between porous plugs and hot metal as 145°, evidently, in water modeling there are wetting conditions meanwhile under industrial conditions there are non-wetting conditions. Thermal expansion due to bubble heating is quite large taking into account that the temperature gradient is in the order of $1873/298 = 6.3$ times.

Porous plugs and not nozzles are employed in industrial ladle furnaces. In water modeling the vast majority of the research work has been carried out with nozzles and only few works with porous plugs. Porous plugs have the potential to produce small bubbles in comparison with nozzles, however, under ladle furnace conditions it can be anticipated nearly constant bubble and liquid velocities in the major portion of the upwelling two phase region, thus, the larger bubble size in industrial conditions resembles more the regime obtained with nozzles. Mazumdar and Guthrie [19] state that the equilibrium distribution bubble size in the fully developed region of the plume is determined by the thermophysical properties of the system and not by the inlet operating variables (gas injection device, orifice diameter, etc.). Bubbles reach an equilibrium bubble size due to both a decrease in hydrostatic pressure and thermal expansion. If the injection device does not have a marked effect on the equilibrium distribution bubble size, then it is to be expected a negligible effect on mixing time. Stapurewicz and Themelis [20] reported experimental evidence of a similar mixing time between porous plugs and nozzles in a water model, independently of the aspect ratio however, Cho *et al.* [21] reported different results. They found for the range from 1-5 l/min, that porous plugs can yield a shorter mixing time only if the aspect ratio is close to 1. When the aspect ratio is close to 0.8, mixing time is similar in both injection devices. The shortest mixing time was found for the aspect ratio of 0.8. Stapurewicz and Themelis investigated mixing time in a large water model, using porous plugs of two sizes (25 and 85 mm) and a nozzle of 10 mm with central injection. The ladle had a diameter of 660 mm. Three aspect ratios were analyzed, 0.67, 0.83 and 1.0. It should be noticed that this comparison is among injection elements of different diameter, furthermore, it is also noticed that the smaller size porous plug was employed only in a few experiments at low gas flow rates.

Whether mixing time is affected by the type of injection device or not, at least in water models, it is a matter which requires further research, however, the small bubble size produced by porous plugs is effective in the removal of non metallic inclusions. Several investigations have concluded that the removal of non-metallic inclusions is enhanced by the smaller bubble size produced by porous plugs [22–24]. Zhang and Taniguchi [23] reported a model which suggests an optimum bubble size, from 1-5 mm, for better efficiency in inclusion removal and also that above 20 mm, bubbles are ineffective in inclusion removal. Wang *et al.* [22] computed bubble size in water (cold) and high temperature systems indicating that the bubble size in liquid steel is twice with respect to that in water. Stapurewicz and Themelis [20] also reported an improved mass transfer coefficient with porous plugs in comparison with nozzles. They obtained a relationship between bubble size and gas flow rate which indicates a larger bubble size as gas flow rate increases. As the gas flow rate increases it also increases gas velocity($\nu_g = Q_g/A_{pp}$). At very high gas velocities (larger than 0.25 m/s) jetting occurs at the porous plug, acting like a nozzle and then mass transfer is reduced.

Bubble size produced by gas injection both in water and liquid steel has been measured ex-

perimentally. Davidson and Amick [25] first proposed two relationships to predict bubble size as a function of gas flow rate using wetted nozzles in water. They indicated that at low gas flow rates the average bubble size is independent of the gas flow rate, depending only on the nozzle size and surface tension of the liquid. At higher gas flow rates depends on both gas flow rate and nozzle size. Sano *et al.* [26] reported experimental data on bubble formation at single non-wetted nozzles. In this work liquid mercury was used as the liquid phase and nitrogen as the gas phase. Their experimental data were in agreement with the correlation by Davidson and Amick if the inner diameter of the orifice is replaced by the outer diameter.

$$d_B = \left\{ \left(\frac{6\sigma d_n}{\rho_l g} \right)^2 + 0.0242 \left(Q^2 d_n \right)^{0.867} \right\}^{\frac{1}{6}} \tag{4}$$

Where; d_B is the bubble diameter in cm, σ is the surface tension of liquid in dyn/cm, d_n is the inner nozzle diameter in cm, ρ_l is the liquid density in g/cm^3, g is the gravitational constant in cm/s^2 and Q is the gas flow rate in cm^3/s.

Mori [27] defined the transition between low and high gas flow regimes for bubbles injected in water and liquid steel as 0.12 l/min and 0.6 l/min, respectively. Irons and Guthrie [28] measured bubble formation at nozzles using hot metal at 1250°C and obtained similar results to those reported by Sano *et al.*. Iguchi *et al.* [29] reported an equation to compute bubble size as a function of the inner nozzle diameter in high temperature systems. The experimental values (14-16 mm) were a little smaller than those predicted by Sano *et al.* (16-19 mm). Hirasawa *et al.* [30] reported bubble sizes in the range of 7-14 mm for molten Cu-molten slag at high temperatures and also an increase in bubble frequency increasing the gas flow rate. Valentin *et al.* [31] built a 1:1 water model, reporting the formation of small bubbles (less than 10 mm) only at low gas flow rates in the order of 1Nm^3/h, above this value they reported coalescence and bubble diameters up to 80 mm at 40Nm^3/h.

Bubble formation with porous plugs has been investigated in some detail however wetting differences between the water model and industrial conditions are usually not addressed. Anagbo and Brimacombe [32–34] investigated gas injection with porous plugs. They found three regimes as gas flow rate was increased. In the first one, bubble frequency increased with increasing the specific gas flow rate up to 8cm^3/(s · cm^2) of the plug surface. This regime was associated with the development of discrete bubbles at the plug, the increasing bubble frequency was attributed to the progressive activation of more pores in the plug with increasing was flow rate. The next region was characterized by a stable value of the bubble frequency, between 8 and 14 cm^3/(s · cm^2), thereafter, the bubbles begin to cluster and coalesce in small pockets, leading to a reduction in bubble frequency. The coalescence regime gradually increased in intensity up to about 40 cm^3/(s · cm^2). Bubble velocity increased from the discrete to the incipient coalescence regime, due to the larger kinetic energy of the injected gas which was found to be proportional to $Q^{0.2}$, however, in the full coalescence regime the velocity decreased. This was attributed to the increased resistance of the liquid phase to the initial motion of the large envelope as well as the loss in kinetic energy of the gas in the process of coalescence. Three regimes were also confirmed in a study by Iguchi *et al.* [35], schematically shown in Figure 2. They also reported that the critical superficial velocity between the low and medium gas flow rate regimes was in the range from 0.14-0.15 m/s. Baxter and Wraith [36] separated in four regimes the different modes of gas dispersion with porous plugs. They defined coalescence from

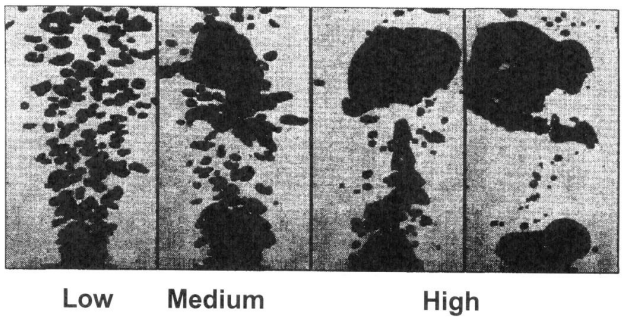

Fig.2 Photographs of gas dispersion in porous plug injection based on ref. [35].

the point where the dispersion resembled that produced by an open orifice. The blanketing regime was characterized by bubbles of the same diameter as the exposed porous plug surface.

If the current limitations of porous plugs to produce small bubbles under industrial conditions still remain and nozzles produce a more representative bubble size, then water modeling with porous plugs appears unjustified. However, water modeling has also provided evidence of the potential benefits of producing small bubbles at least in terms of mass transfer, removal of non metallic inclusions and even on mixing. The problem still unsolved is how to create small bubbles in industrial conditions. Several investigations [37–40] have been focused on using vibrations to create small bubbles. The bubble size has been reported to be one half with ultrasonic vibration in comparison with the conventional method. This tool is also been used in the industry to control bubble stirring [41–43]. In practice bubble stirring cannot be controlled efficiently with gas flow meters due to clogging of porous plugs.

4 Optimum configuration of injection elements

Fluid flow optimization in steel ladles requires the definition of the optimum number and location of injection devices. For the purpose of obtaining the understanding of the phenomena involved, many physical and mathematical models have been developed with a number of limitations. In order to decide the optimum configuration following variables should be considered: number of injection elements as a function of ladle dimensions, radial distance from the center, separation angle, gas flow rate, mixing time, thermal expansion of gas bubbles, wettability, ladle eye area, refractory erosion and mass transfer coefficient. Evidently it would be an extremely difficult task to involve all the operational variables. Perhaps this explains why there is no universal agreement about the optimum number and location of injection devices [44–53]. Most of the experimental investigations suggest a location at half radius and two porous plugs, however there is large disagreement with respect to the separation angle. Most of this research work has been carried out without the presence of slag and only few investigations have analyzed radial distances larger than half radius. It is required more research involving radial distances closer to the wall.

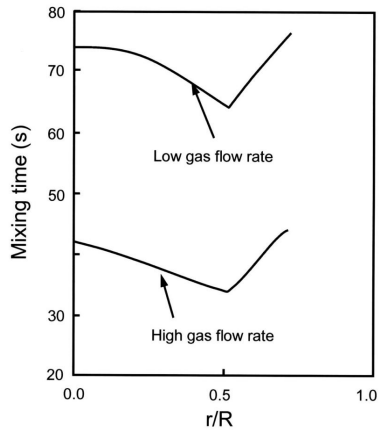

Fig.3 Effect of radial position on mixing time based on ref. [44].

Joo and Guthrie [44] reported physical and mathematical modeling of gas injection in a one-third scale water model of a 100t industrial ladle. Slag was not included in

the analysis. Several positions of the injection elements were considered from 0 to $0.67R$. Figure 3 schematically shows their result and it clearly defines the influence of both position and gas flow rate of one single tuyere. This research also provides experimental data comparing one and two tuyeres, indicating that a dual configuration yields shorter mixing times than a single tuyere. The separation angle of was also analyzed with two tuyeres. It was found a shorter mixing time when the tuyeres are separated 180°. It was argued that that when the two tuyeres are closely placed, the plumes coalesce, diminishing the effect of double gas bubbling. When the tuyere is moved away from the center, solute transport by angular momentum increases.

Several investigations have relied upon the mathematical modeling and excluding the top layer to define the optimum configuration [45–47]. Pan *et al.* [45] reported an optimum configuration with 3 porous plugs located at 0.25 R. They didn't provide experimental evidence to support their results. Zhang *et al.* [46] reported a mathematical model which describes the influence of the separation distance between two nozzles at 180° separation angle. Their model was partially validated with experimental data from another publication. They concluded that two nozzles at half radius and 180° separation angle, the mean energy dissipation rate is maximum, however, this result was not supported by experimental work, furthermore, separation distances beyond half radius were not investigated. Jauhiainen *et al.* [47] reported a mathematical model analyzing the position of 2 nozzles in 4 different arrangements simulating an industrial ladle of 110t. They evaluated the separation angle and distance away from the center. The four nozzle configurations involve 2 nozzles separated 60° at $0.5R$ and $2/3R$, 2 nozzles separated 180° at $0.5R$, and the 2 nozzles in the center. The standard deviation from the mean concentration as a function of time was used as the criteria to define the best configuration in order to get better mixing. They concluded that the central position renders the best mixing, however, this location is particularly sensitive to tracer addition position, and then, their final suggestion was that 2 nozzles at half radius and with 60° separation is the best option. No experimental data was provided to validate their model.

Mazumdar *et.al.* [48,49] investigated mixing time for a dual nozzle arrangement. This research employed a fixed position of the two nozzles. They evaluated the influence of the aspect ratio and gas flow rates. The relationship reported for mixing time, valid for dual nozzle configuration and a tapered vessel is the following:

$$\tau_m = 15 Q^{-0.38} H^{-0.5} R_{eff}^{2.0} \tag{5}$$

Where: τ_m represents mixing time in seconds, Q is the gas flow rate in m^3/s, H is the height of liquid in meters, R_{eff} is the effective radius of the tapered vessel in meters.

Recently, Zhang *et.al.* [50] conducted physical and mathematical modeling for a 120t ladle at 1:3 scale. They analyzed three positions but details of the exact location were not provided. This investigation concludes that the shortest mixing time is achieved when three nozzles are in operation.

Chen *et al.* [51], reported a detailed work which includes for the first time a dual configuration in the presence of a top layer. The work appears to be quite complete since multiple arrangements were investigated, including separation angle and distance away from the center. The standard configuration employed in a 150t ladle corresponds to two nozzles separated 60°, one nozzle is placed at 0.67 R and the other one at $0.79R$. Figure (4a) describes mixing time as a function of gas flow rate and nozzle separation angle. It is observed that a separation angle of 45° yields

the shortest mixing time, especially at the lower end of the gas flow rate. As the gas flow rate increases, the influence of the separation angle is less important. Figure (4b) reports the analysis of several configurations changing the position of the nozzles. The configuration with the two nozzles placed at half radius gave the shortest mixing time, however, a configuration with two nozzles placed at $2/3R$ was not included in this analysis.

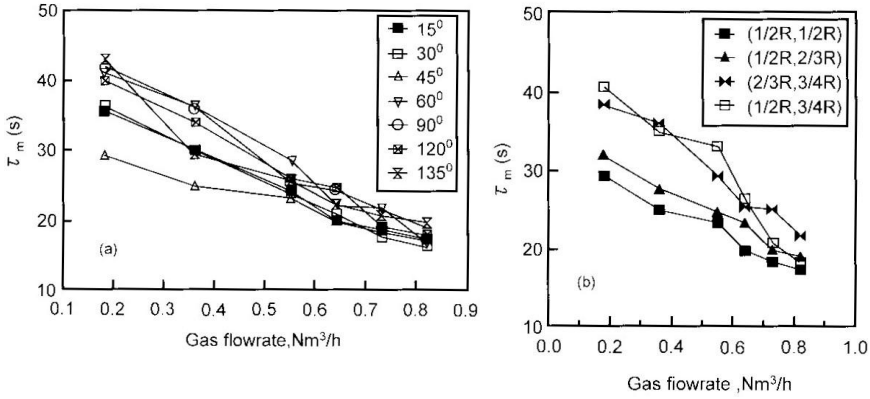

Fig.4 Mixing time as a function of nozzle separation angle and nozzle configuration [51].

Few investigations, based on physical and mathematical modeling, have suggested only one porous plug to minimize mixing time [52, 53]. Zhu *et. al.* [52] compared mixing time with one, two and three tuyeres and the shortest mixing time was found with one tuyere eccentrically located. In this work six types of tuyere arrangement were investigated, varying position and separation angle. The water model represented a 350t ladle, with a scale of 1:10. They reported a gas flow rate for the industrial ladle in the range of 21-48 Nm^3/h. The gas flow rate in the model ranged from 4-8 l/min. For a better flow visualization, alumina particles of 0.2 mm diameter were employed. Figure 5 describes the mixing time as a function of the six configurations. From this figure is evident that one single tuyere, eccentrically located, yields the shortest mixing time.

The previous results were expressed with the following relationship, which indicates that increasing the number of porous plugs, increases mixing time.

$$\tau_m = 8.52\varepsilon_m^{-0.33} N^{0.33} \tag{6}$$

Where: τ_m represents mixing time in seconds, ε is the specific stirring energy in watts/kg, N is the number of tuyeres.

The exponent in the number of tuyeres(N) agrees with another relationship previously reported by Nakanishi in 1982 $\left(\tau_m = 800\varepsilon_m^{-0.4} N^{0.33}\right)$. More recently Ramirez-Argaez [53] derived a relationship from mathematical modeling which also suggests the shortest mixing time with one tuyere:

$$\tau_m = 3.41 W^{0.3} Q^{-0.25} N^{0.4} \left(r/R\right)^{-0.12} \left(H/D\right)^{-0.44} \tag{7}$$

Where: τ_m represents mixing time in seconds, W represents mass in kg, Q is the gas flow rate in l/s, r/R is the fractional position away from the center, H/D is the ratio between height of liquid to the diameter and N the number of tuyeres.

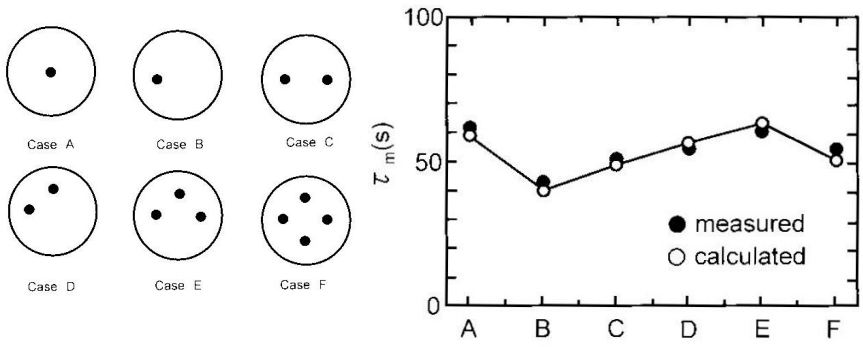

Fig.5 Mixing time as a function of number and position of tuyeres [52].

Table 2 summarizes the optimum configuration in terms of number of tuyeres, separation angle and radial distance away from the center (r/R).

Table 2 Optimum design for a dual nozzle configuration.

		Experimental conditions			Optimum values		
Year	Author	Top layer	N	r/R	N	r/R	θ°
1992	Joo and Guthrie [44]	No	1,2	0,0.3,0.5,0.67	2	0.5	180°
1995	Zhu *et. al.* [45]	No	1,2	1 T: 0, 0.5 2 T: 0.5(180°), 0.5(90°) 3 T: 0.5(90°) 4 T: 0.5(90°)	1	0.5	-
1997	Pan *et. al.* [46]	No	1,2,3	0,0.25,0.33	3	0.5	120°
2000	Zhang *et. al.* [47]	No	2	0.06, 0.2, 0.33, 0.5	2	0.5	180°
2001	Jauhiainen *et. al.* [48]	No	2	0, 0.25, 0.67	2	0.5	60°
2004	Madan *et. al.* [49]	No	2	0.5	-	-	-
2005	Mandal *et. al.* [50]	No	2	0.5	-	-	-
2007	Chen *et. al.* [51]	Yes	2	0.5,0.66,0.75,0.79	2	0.5	45
2008	Zhang *et. al.* [52]	No	1,2,3	-	3	-	-

The selection of a top layer which fulfills dynamic similarity seems to be a difficult task. In the past, the selection of a top layer in water modeling research has been carried out without a proper analysis of this requirement. In many cases, top layers of low density have been selected, with density ratios closer to 1. The realistic value is about 2.2. Some investigations have been carried out with realistic density ratios, however the changes in the properties of the fluids affect any measurement of mixing time. The authors are currently analyzing the influence of both density and viscosity changes of the top layer on mixing time [54].

5 Conclusions

In the past 35 years a large body of knowledge on fluid flow phenomena has been accumulated which has been used to improve the ladle furnace process. In spite of this enormous progress there are issues which still require additional research in order to improve the current limitations

in both physical and mathematical modeling, such as involving the top layer, scale up laboratory data to industrial conditions and get a general agreement about the optimum configuration of injection devices, expressed in terms of number and location. Another important aspect in bubble stirring is the necessity to produce small bubbles in industrial conditions, overcoming the current limitations due to poor wettability between the porous plug and liquid steel. The use of ultrasonic vibrations to produce small bubbles appears as a promising tool to enhance the efficiency of porous plugs in industrial conditions.

文 献

[1] Mazumdar D.; Met. Trans. B., **21B** (1990) 925-928.

[2] Hsiao T-C, Lehner T. and Kjellberg B.; Scand. J. Metallurgy, **9** (1980) 105-110.

[3] Sahai Y. and Guthrie R.I.L.; Met. Trans. **13B** (1982)193-202.

[4] Sahai Y. and Guthrie R.I.L.; Met. Trans., **13B** (1982) 203-211.

[5] Mazumdar D., Guthrie R.I.L. and Sahai Y.; Appl. Math. Modelling, **17** (1993) 255-262.

[6] Mazumdar. D.; Met. Trans. **33B** (2002) 937-941.

[7] Mazumdar D. and Guthrie R.I.L.; Met. Trans., **16B** (1985) 83-90.

[8] Kim S. and Fruehan R.J. Met. Trans. **18B** (1987) 381-390.

[9] Sudhakar V. and Mazumdar D.; Met. Trans., **27B** (1996) 704-708.

[10] Mazumdar D. Kim H.B. and Guthrie. R.I.L.; Ironmaking and steelmaking, **27** (2000) 4, 302-308.

[11] Mazumdar D. and Guthrie R.I.L.; Iron and steelmaker (ISS Trans), September 1999, 89-96.

[12] Mazumdar D. and Guthrie R.I.L.; Met. Trans., **17B** (1986) 725-733.

[13] Neifer M., Rodl S. and Sucker D.; Steel research, **64** (1993) 1, 54-62

[14] S.Asai, T.Okamoto, J.He and I. Muchi.; Trans. ISIJ, **23** (1983) 43-50.

[15] K. Ogawa and T. Onoue.; ISIJ Int., **29** (1989) 2, 148-153.

[16] Abel C., Fruehan R. and Vassilicos A.; Trans ISS, I&SM, July 1995, 47-56.

[17] Shin-Ya Kitamura and Tadamasa Yajima. Personal comunicación. Kawatabi seminar. August 2009.

[18] Wang Z., Mukai K. and Izu D.; ISIJ Int., **39** (1999) 2, 154-163.

[19] Mazumdar D. and Guthrie R.I.L.; ISIJ Int., **35** (1995) 1, 1-20.

[20] Stapurewicz T. and Themelis N.J.; Can. Met. Q., **26** (1987) 2, 123-128.

[21] Cho S., Kim C., Han J., You B. and Kim D.; Mat.Sc. Forum, **vols 510-511** (March 2006), 494-497.

[22] Wang L., Lee H-G. and Hayes P.; ISIJ Int., **36** (1996) 1, 17-24.

[23] Zhang L. and Taniguchi S.; Int. Mat. Reviews, **45** (2000) 2, 59-82.

[24] Zheng S. and Zhu M.; Acta Met. Sinica, **42** (2006) 11, 1143-1148. (in Korean).

[25] Davidson L. and Amick E.H.: AIChe J., 1956, p.337

[26] Sano M., Fujita Y. and Mori K.; Met. Trans., **7B** (1976) 300-301.

[27] Mori K.; Trans. ISIJ, **28** (1988) 246-261.

[28] Irons G.A. and Guthrie R.I.L.; Met. Trans., **9B** (1978) 101-110

[29] Iguchi M., Kawabata H., Nakajima K. and Morita Z.; Met. Trans., **26B** (1995) 67.

[30] Hirasawa, M., Mori K., Sano M., Hatanaka A., Shimatani Y. and Okazaki Y., Trans. ISIJ, **27** (1987), 277-282.

[31] Valentin P., Bruch C., Kyrylenko Y. Kochner H. and Dannert C.; Steel Res. Int., **80** (2009) 8, 552.
[32] Anagbo P.E. and Brimacombe J.K.; I&SM, October 1988, 38-43.
[33] Anagbo P.E. and Brimacombe J.K.; I&SM, November 1988, 41-45.
[34] Anagbo P.E. and Brimacombe J.K.; Met. Trans., **21B** (1990) 637.
[35] Kaji M., Sawai T. and Iguchi M.; Mem. School. BOST Kinki University, **4** (1998) 1-12.
[36] Baxter R. and Wraith A.; Chem.Eng. Sc., **25** (1970) 1244-1247.
[37] Kawakami K., Tono N., Douwaki S. and Ito K.; Testu-to-Hagane, **76** (1990) 6, 856-862
[38] Kawakami K., Douwaki S., Hiroe T. and Ito K.; Testu-to-Hagane, **78** (1992) 5, 745-752.
[39] Kobayashi M., Kamata C. and Ito K.; ISIJ Int., **37** (1997) 1, 9-15.
[40] Okumura K. and Hayashi S.; Proceedings Asia Steel 2009, Busan Korea, May 24-27, 2009.
[41] Minion R.L., Leckie C.F., Legeard K.J. and Richardson B.D.; Iron and Steelmaker, **25** (1998) 7, 25-31.
[42] Kemeny F., Walker D. and Jones J.; U.S. Patent 6 264 716, July 24, 2001.
[43] Lee S., Byun S-M., Park J., Suk M-O., Jones J. and Walker D.; Scanmet III, 3rd International conference on process development in iron and steelmaking, June 8-11, 2008, Lulea Sweden. 131-140.
[44] Joo S. and Guthrie R.I.L.; Met. Trans.B., **23B** (1992) 765-778.
[45] Pan S., Ho Y. and Hwang W.; J. Matls. Eng. and Performance, **6** (June 1997) 3, 311-318.
[46] Zhang L., Taniguchi S., Cai K. and Qu Y.; Steel research, **71** (2000) 9, 325-332.
[47] Jauhiainen A., Jonsson L. and Sheng D.; Scand. J. of Metallurgy, **30** (2001) 242-253.
[48] Madan M., Satish D. and Mazumdar D.; ISIJ Int., **45** (2005) 5, 677-685.
[49] Mandal J. Patil S., Madan M. and Mazumdar D.; Met. Trans B., **36B** (2005) 479-487.
[50] Zhang Ge, Chen Z. and Xu Y.; ICS 2008, 335-338.
[51] Chen M. Wang N. Yao Y. Geng J. and Xiong K.; Steel research int., **78** (2007) 6, 468-472
[52] Zhu M., Inomoto T., Sawada I. and Hsia T.; ISIJ Int., **35** (1995) 5, 472-479.
[53] Ramirez-Argaez, M. Matls. and Manuf. Processes, **23** (2008) 59-68.
[54] Conejo A.N., Kitamura S., Iguchi M., Maruoka, N. and Kim S. Unpublished research. 2009.